Effects of Energetic Electron and Proton Irradiation on Electron Emission Yield of Polyimide Induced by Electron and Photon

Effects of Energetic Electron and Proton Irradiation on Electron Emission Yield of Polyimide Induced by Electron and Photon

By Jiang WU[1, 2)], Akira MIYAHARA[1)], Arifur KHAN[1)],
Minoru IWATA[1)], Kazuhiro TOYODA[1)], Mengu CHO[1)] and Xiaoquan ZHENG[2)]

[1)]*Kyushu Institute of Technolgy, Kitakyushu, Japan*
[2)]*State Key Lab of Electrical Insulation and Power Equipment, Xi'an Jiaotong University, Xi'an, China*

As the electron emission yield induced by electron and photon plays a key role in surface potential of spacecraft materials, the ground based degradations including 500 keV electron and 50 keV proton irradiation with 4 different fluences were conducted for the polyimide film separately. Based on the developed measuring systems, the comparative measurements of total electron emission yield and photoelectron emission yield were carried out for the virgin and degraded polyimide samples respectively. The total electron emission yield and photoelectron emission yield tended to have different variation tendency after high energy electron and proton irradiation. The Monte-Carlo analysis software Casino and SRIM were used to analysis the distribution and stopping power of electron and proton respectively. According to the measurement results and analysis, the free radicals caused by irradiation was considered to be the main effect for polyimide films, which can primarily reveal the degradation mechanism of energetic electron and proton on the emission yield of polyimide.

Key Words: Total Electron Emission Yield, Photoelectron Emission Yield, Electron and Proton Irradiation, Degradation Effect, Polyimide

Nomenclature

σ	:	total electron emission yield
δ	:	secondary electron emission yield
Y	:	photoelectron emission yield
Subscripts		
max	:	maximum
p	:	primary

1. Introduction

According to the current balance equation, the electron emission yield of the spacecraft surface materials plays the crucial role in spacecraft potential, especially the total electron emission yield (TEEY) and photoelectron emission yield (PEY)[1,2)]. As the impact of fast moving electrons in the ambient plasma, the long-term operation of spacecraft will gradually lead to the big potential difference on the surface boundaries because of different electron emission property. Usually the weakest part, the triple-junction (conductor, insulator and vacuum), will initiate discharge or even arcing phenomenon, which will damage the spacecraft seriously. Therefore, in order to take use of the MUSCAT for surface potential calculation, at least the database of the TEEY and PEY for various spacecraft surface materials is necessary.

However, the spacecraft is not only influenced by the orbital high density and low energy plasma, but also the space exposure and other degradation. Especially, the long-term operating spacecraft in Geosynchronous orbit (GEO) will suffer the high energy electron and proton irradiation from space. The energetic particles can induced not only the single electron effect and total ionizing dose effect, but also the degradation on surface materials. For the spacecraft surface materials, the above two factors will influence its electron yield, thus the charging property of the spacecraft may vary.

As a kind of spacecraft thermal control materials, the polyimide (PI) film possesses high insulation and well thermal performance and is widely used in the spacecraft body and solar array. Based on the long-period developed TEEY and PEY measurement system, the TEEY and PEY of the virgin polyimide films, electron and proton exposed polyimide films for 4 doses, which are equivalent to 1, 5, 10, 15 years orbital exposure, were investigated.

2. Electron Emission Yield Definition

2.1. Total Electron Emission Yield

The total electron emission yield is defined as the number ration of emitted electrons and injected electrons (primary electrons) with certain primary energy and angel. The curve of TEEY with respect to primary electron energy in normal injection situation is shown in Fig. 1. The universal curves exist for all solid materials, the shape of which depends on 4 key parameters, namely the first and second crossover energy, E_1 and E_2, where the yield reaches unity, and the maximum value of the yield and its related energy, σ_{max} and E_{max}[3)].

The total electron emission includes the secondary electron and backscatter electron. Yet the backscatter electron are less and weak relationship with primary electron energy, the TEEY and SEY usually have the same property.

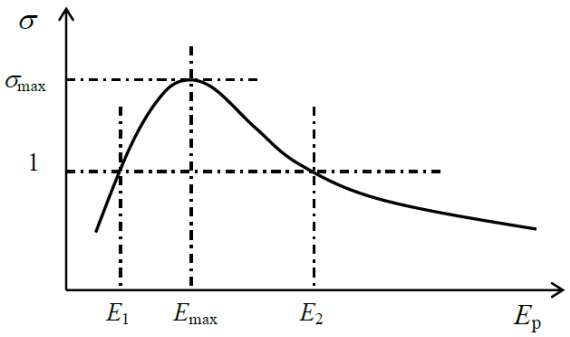

Fig. 1 Universal curve of total electron emission yield of solid materials.

2.2. Photoelectron Emission Yield

The photoelectron emission yield represents the number ratio of outgoing electron to the incident photon. The PEY varies with the incident photon energy or wavelength, the calculation equation expresses as follow[2].

$$\frac{I_{photoelectron}}{S} = q_e \cdot \int_0^{\infty} PF(\lambda) \cdot Y(\lambda) d\lambda \qquad (1)$$

where $Y(\lambda)$ is the PEY of the certain material, $I_{photoelectron}$ is the photoelectron emission current, S is the light beam area, $PF(\lambda)$ is the photo flux, q_e is the unit charge.

3. Experimental Preparation

3.1. Sample Pretreatment

The TORAY DuPont Inc. (Japan) manufactured Kapton 100H type polyimide film with 25 μm thickness were chosen as research object. The film was cut to be 35 mm × 35 mm square shape, and ultrasonically cleaned by alcohol in advance. Before the TEEY or PEY testing, the backside of the samples were coated with Au as the electrode by the SANYU Electronics Inc. (Japan) QC-701 type Quick Coater, and electric potential of the testing side was checked by the TREK Inc. (USA) 362A type Electrostatic Voltmeter. If the potential is higher than ±5 V, the Omron Inc. (Japan) ZJ-FA20 type Ionizer was used to neutralize the surface and eliminate the effect of charging.

3.2. Total Electron Emission Yield

The TEEY measurement system was developed on the base of JEOL JAMP-10 SXII Auger Microscope with a cylindrical metal collector. The chamber, with 7.0×10^{-5} Pa vacuum, is mounted the LaB_6 electron gun, which can emit the primary electron with energy ranging from 10 eV to 10 keV, 20 nA current, 30 μs pulse and 1mm^2 beam spot. The system can measure the TEEY of all solid plate samples with thickness less than 2.5 mm. The system schematic is shown in Fig. 2. Comparing to the sample, the collector is biased to +50 V, in order to catch all the secondary electrons escaping from the sample surface[4].

In the TEEY system, when the primary electron hits the sample surface, the collector and sample current is measured simultaneously and then the yield σ can be calculated as follow.

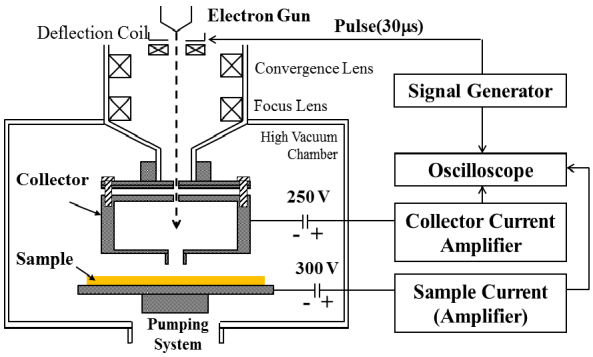

Fig. 2 Schematic of total electron emission yield system.

$$\sigma = \frac{N_{out\_electron}}{N_{in\_electron}} = \frac{I_{collector}}{I_{primary}} = \frac{I_{collector}}{I_{collector} + I_{sample}} \qquad (2)$$

To calibrate the measurement system, the TEEY of gold material was tested. The Fig. 3 shows the experimental results by red circles and comparison with reference data[5].

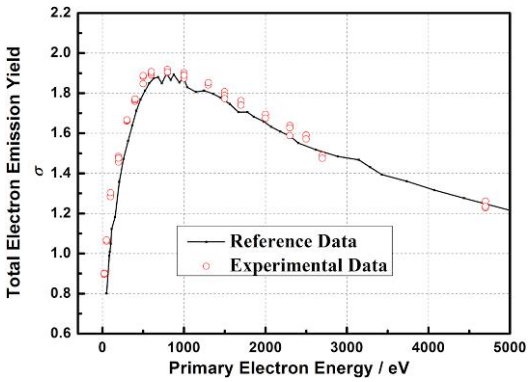

Fig. 3 TEEY system calibration by gold material.

3.3. Photoelectron Emission Yield

The photoelectron emission yield system includes the vacuum system, the compressor, the HAMAMATSU Inc. (Japan) Model L1835 Deuterium Lamp, with wavelength ranging from 115 nm to 400 nm, and the HAMAMATSU Inc. Model H8496-16 UV Laser Sensor with spectral response from 160 nm to 220 nm. The system schematic is depicted in Fig. 4, while Fig. 5 shows the relative intensity of the D2 lamp. The five narrow band filters were used for the incident photon, and their transmittance property was shown in Fig. 6. In the

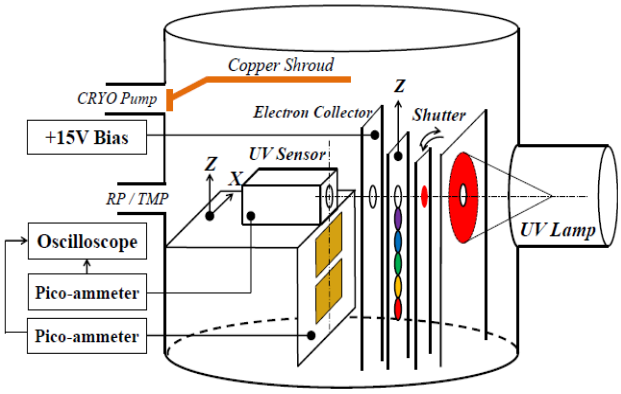

Fig. 4 Schematic of photoelectron emission yield system.

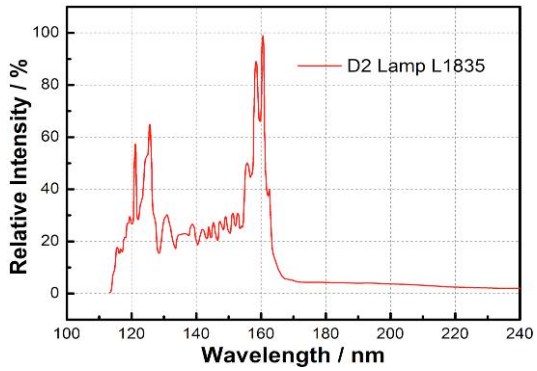

Fig. 5 Relative intensity of D2 lamp L1835.

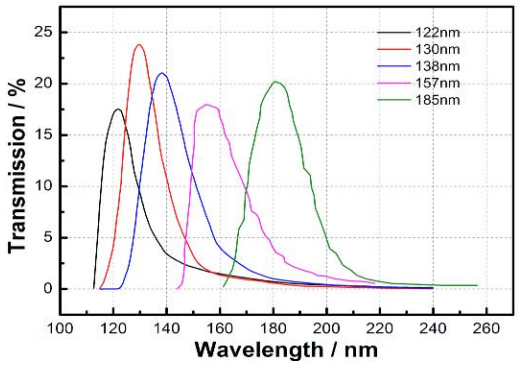

Fig. 6 Transmittance Property of Five Narrow Band Filters.

measurement system, the motor driven shutter is used to control the light pulse, with the pulse width around 200 ms. The sample plate is grounded while the collector is biased to +15 V for photoelectron receiving[6].

As the UV light passes through the filters, the photo flux distribution will depend on the filter property. For calculating the photo flux acts on the sample, the filter property $NBF(\lambda)$ should be added to the right side of Eq. (1), then it turns to

$$\frac{I_{photoelectron\_n}}{S} = q_e \cdot \int_0^{\infty} PF(\lambda) \cdot Y(\lambda) \cdot NBF_n(\lambda) d\lambda \qquad (3)$$

where n=1~5, represents the five filter situations. In order to calculate the $Y(\lambda)$ in Eq. (3), we assumed the double exponential function as:

$$Y(\lambda) = Y_0 + A_1 e^{(\lambda_0 - \lambda)/t_1} + A_2 e^{(\lambda_0 - \lambda)/t_2} \qquad (4)$$

where Y_0, A_1, A_2, t_1, t_2, λ_0 are the six parameters. Taking Eq. (4) back to Eq. (3), we can obtain the five calculated photoelectron currents, which then are compared with the experimental photoelectron current under five different filter situations respectively. And the difference Δ between these two types of currents is defined as follow.

$$\Delta = \sum_{n=1}^{5} \left(\frac{I_{calculated\_n}}{I_{experimental\_n}} - 1 \right)^2 \qquad (5)$$

When the difference Δ reaches minimum, then the best value for the six parameters are obtained, also the PEY property.

Based on this simulation method, we measuremed the gold material to calibrate the system as shown in Fig. 7. The

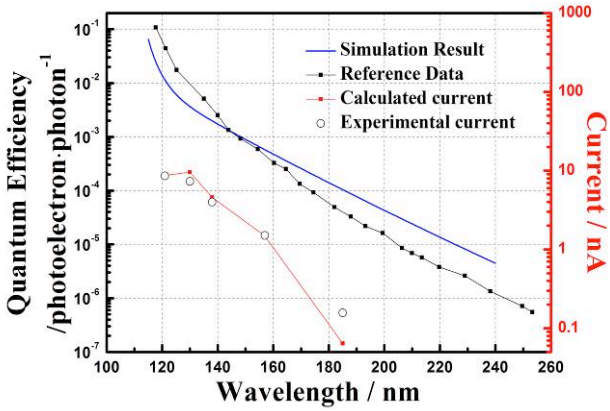

Fig. 7 PEY system calibration by gold material.

calculated photoelectron current from simulated PEY and experimental photoelectron current is also compared in Fig. 7[7].

3.4. Solutions For Surface Charging

In the case of insulation material, the surface charging will influence the electron emission yield, as the generated electron will be trapped by the surface potential. In order to solve this problem, two solutions are proposed for both systems. Firstly, during the measurement the sample moves step by step, and Fig. 8 illustrates the measuring positions on sample, and each position is only measured for one electron or photon shot. Secondly, we used the pulse control for each electron or photon shot. The pulse width is around 30 μs and 200 ms for TEEY and PEY system respectively.

Figure 9 and 10 show the typical current waveform of the

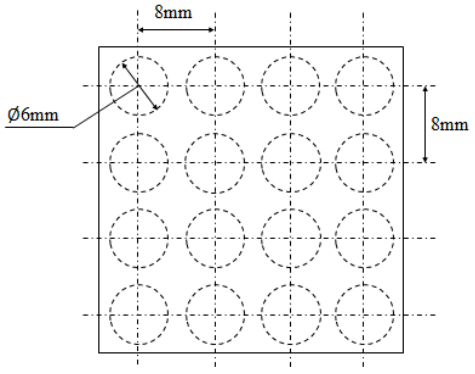

Fig. 8 Measurement position on sample for scanning method.

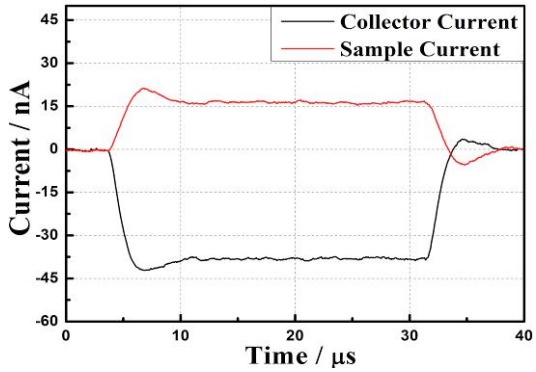

Fig. 9 TEEY current waveform of polyimide at 150 eV.

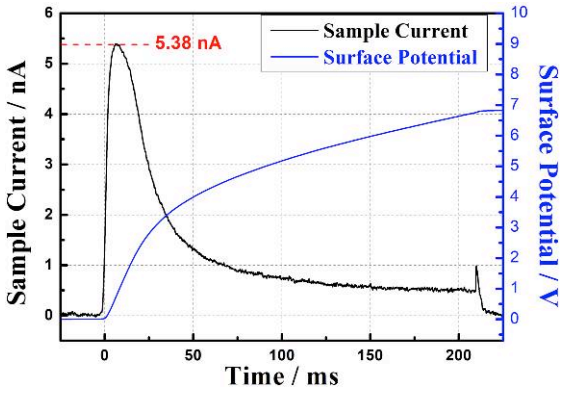

Fig. 10 PEY current waveform of polyimide at 122 nm filter situation.

TEEY and PEY of polyimide respectively. From Fig. 9, the current waveform's flatness proves that the surface charging is not obvious; while for PEY measurement current wavelength of polyimide shown in Fig. 10, the surface charging occurred and the surface potential is around +7 V. However, as the collector in PEY system is biased to +15 V, we consider that the photoelectron can still escape from the sample surface.

3.5. Energetic Electron and Proton Irradiation

The pretreated virgin polyimide films were irradiated by the energetic electron and proton beam separately for single effect investigation.

The high energy electron irradiation test was carried out at Takasaki Advanced Research Institute, Japan Atomic Energy Agency (JAEA). The perpendicular injecting electrons with 500 keV energy and 0.5 mA beam current was chosen for 4 different irradiation periods, which represented the fluence of 9.3×10^{14}, 4.7×10^{15}, 9.3×10^{15} and 1.4×10^{16} electron/cm^2 and equivalent to 1, 5, 10, 15 years exposure dose in GEO respectively.

On the other hand, the proton irradiation test was performed at The Wakasa Wan Energy Research Center. The perpendicular injecting protons with 50 keV energy and 1 μA/cm^2 beam density was chosen for 4 doses of 5.3×10^{14}, 2.7×10^{15}, 5.3×10^{15} and 8.0×10^{15} proton/cm^2 and equivalent to 1, 5, 10, 15 years GEO exposure respectively.

After the beam exposure, the samples were all kept in vacuum before any test, which intended to prevent the air exposure effect. The periods between irradiation and measurement of the TEEY and PEY are listed in Table 1.

Table 1. Periods between irradiation and measurement (in vacuum).

Period / day	TEEY	PEY
Electron	7	7
Proton	10	1

4. Experimental Results

4.1. Total Electron Emission Yield

Due to the material dispersion, TEEY results of virgin polyimide measured at room temperature by several groups were averaged and is shown in Fig. 11(a), comparing with the reference[8]. Table 2 shows the key parameters for the TEEY of polyimide film.

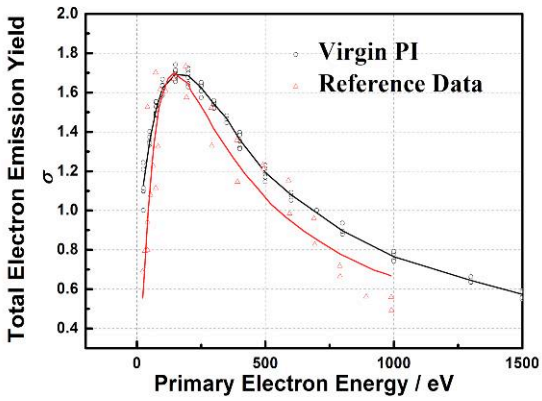

(a)

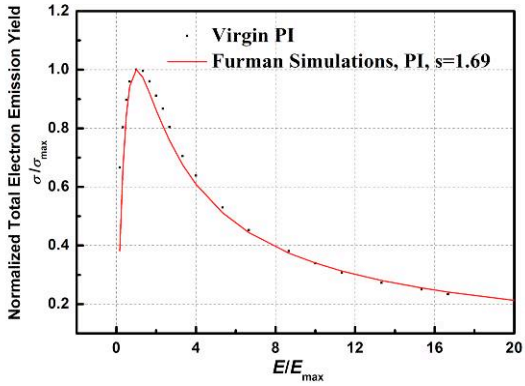

(b)

Fig. 11 TEEY curves of virgin polyimide films (a) TEEY of virgin polyimide film and reference data (b) normalized TEEY of virgin polyimide and Furman simulation.

Table 2. Comparison of TEEY key parameters of virgin polyimide.

	E_2 (eV)	E_{max} (eV)	σ_{max}
Experimental Data	670	150	1.69
Reference (7)	500	150	1.7

Since SEEY is the dominant channel in TEEY, behavior pattern of TEEY is similar to SEEY. According to the simulation theory of SEEY by Furman[9], the relationship between the electron yield and primary electron energy is as expressed in Eq. (6).

$$\delta(E_p) = \delta_{max} \cdot \frac{s\cdot(E_p / E_{max})}{s-1+(E_p / E_{max})^2} \qquad (6)$$

where, the E_p is the primary electron energy, δ_{max} is the maximum value of SEEY, E_{max} is the primary electron energy at δ_{max}, and s is the related coefficient ranging from 1 to 2 for solid material. Using Eq. (6) and the data in Table 2, the TEEY of polyimide film was simulated, normalized, and displayed in Fig. 11(b).

Figure 11 infers that the experimental data is identical with the reference and the Furman simulation results. The TEEY of electron and proton irradiated polyimide films are shown in Fig. 12.

From Fig. 12(a) we can conclude that the total electron emission yield rises, especially for the σ_{max} from 1.7 to near

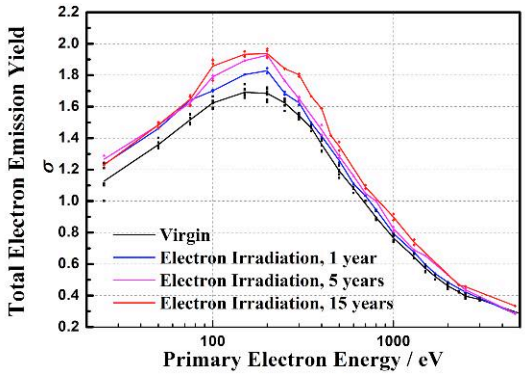

(a)

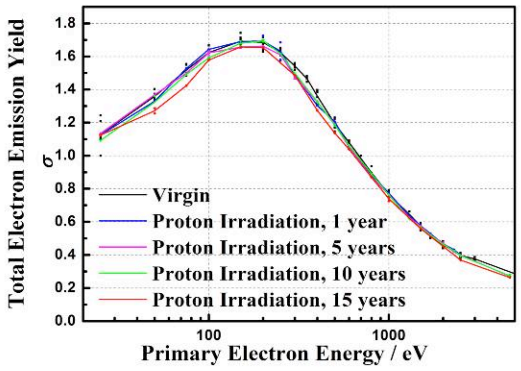

(b)

Fig. 12 TEEY of exposed polyimide films (a) 500 keV electron (b) 50 keV proton.

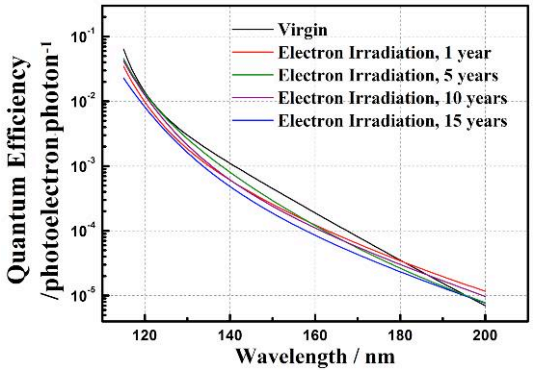

(a)

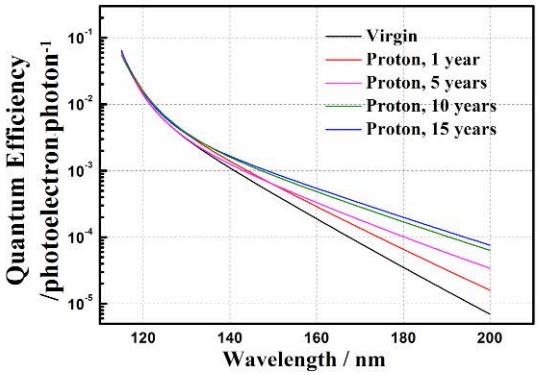

(b)

Fig. 14 PEY of exposed polyimide films (a) 500 keV electron (b) 50 keV proton.

2.0, with the electron irradiation fluence increasing, while the E_{max} keeps invariant; for the proton irradiation samples, the TEEY slightly decreases from virgin one as shown in Fig. 12(b). However, taking the material dispersion into consideration, we consider that the TEEY maintains after proton exposure.

4.2. Photoelectron Emission Yield

The PEY tests of virgin PI were firstly conducted in this research. Using the double exponential simulation method explained in Section 3.3, we calculated the PEY property based on the experimental results. Fig. 13 shows the PEY of virgin polyimide films, reference data and the current comparison.

The Figure 14(a) shows that, the photoelectron emission yield decreases with the electron irradiation dose rising, while the PEY of proton irradiated polyimide films increases with the dose rising as depicted in Fig. 14(b). Especially in Fig. 14(b), the PEY rising more significantly at long wavelength photon bombardment.

5. Discussion and Analysis

Based on the previous results, the space environmental energetic electron and proton irradiation has significant effect on the electron emission yield of polyimide film.

In order to further clarify the tendency of photoelectron emission of polyimide film and get the actual use of PEY, we can calculate the photoelectron emission current density under certain space environment. Suppose the spacecraft is operated at the top of the atmosphere, where the solar spectrum was

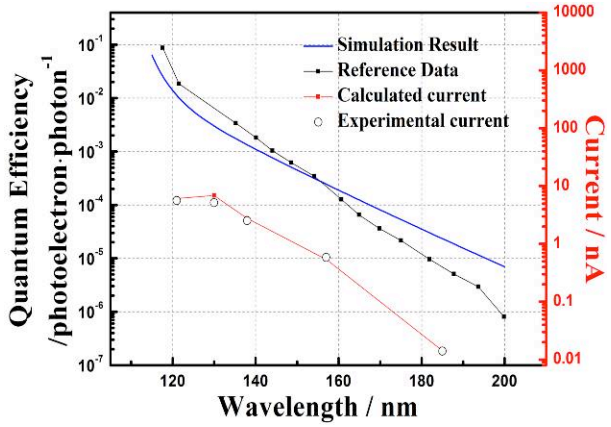

Fig. 13 PEY of virgin polyimide film and reference data

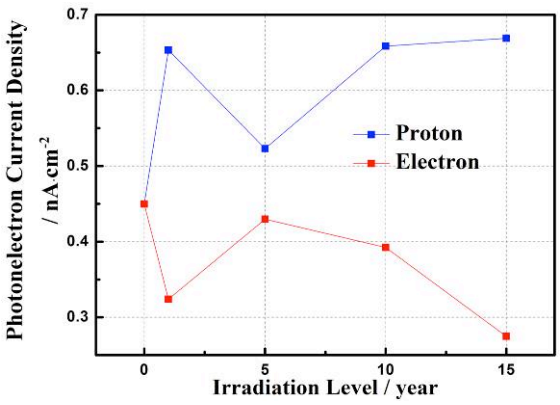

Fig. 15 Photoelectron current density of irradiated polyimide films under AM0 solar spectrum.

known as the AM0 distribution, and the polyimide film upon the spacecraft faces to the sun, which means the perpendicular injection for the photons to the polyimide film. The current density of virgin polyimide, electron and proton irradiated polyimide was all calculated and shown in Fig. 15.

Figure 15 refers that, under single effect of electron and proton irradiation, the photoelectron emission current density goes to the opposite direction. The current density for 1 year equivalent irradiation of both factors seems to vary too significantly, however, the tendency still shows rising for proton irradiation and decreasing for the electron irradiation, respectively.

In order to analyze the degradation phenomenon, we used the public software Casino v2.48 and SRIM-2013 to calculate the transportation property of the electron and proton in polyimide film respectively. For the proton calculation, the proton beam, with 10^5 protons, was set to be 50 keV and perpendicular to the surface of the polyimide film. Figure 16 shows the simulation results, which infers that, the average depth for proton is around 600 nm in Fig. 16(a). Meanwhile, the stopping power, which presents the energy loss of the incident particles per unit distance, was also calculated from 10 keV to 200 keV protons irradiated to polyimide film shown in Fig. 16(b). It inferred that, the protons with energy around 75 keV give the maximum stopping power. However, after the proton injected into the material, their stopping energy will vary due to the energy loss of themselves. Usually, the stopping power exists a peak before the particles finally trapped in the material, which can be confirmed by the 100, 150 and 200 keV proton in Fig. 16(c). Due to the low energy, 50 keV protons lose all their energy to the very surface zone. According to the above two point, we can conclude that the 50 keV proton induced high ionization in the polyimide surface layer, where the secondary electron and photoelectron is considered to be generated.

For the electron calculation, the electron beam, with 10000

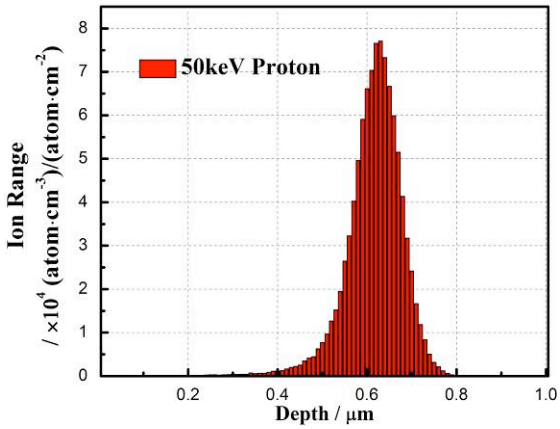

(a)

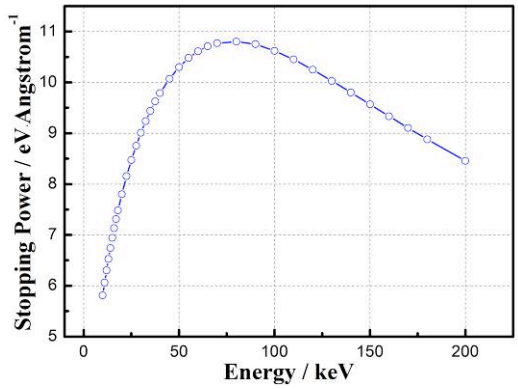

(b)

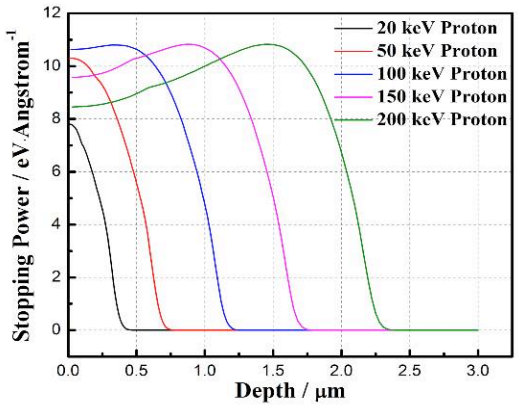

(c)

Fig. 16 Simulation of proton distribution and stopping power in polyimide film by SRIM (a) distribution (b) stopping power with energy (c) stopping power with depth.

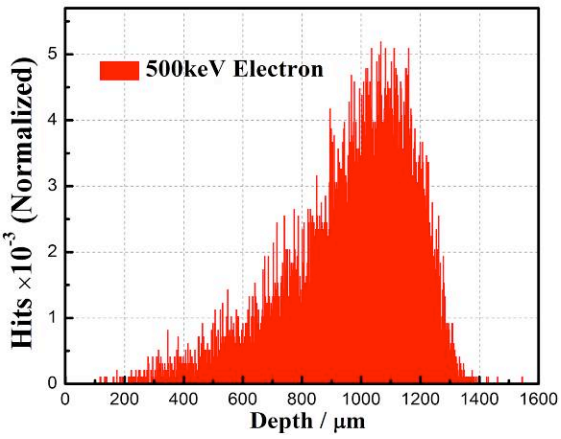

(a)

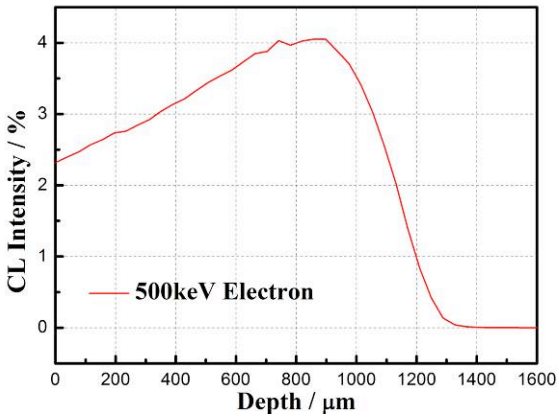

(b)

Fig. 17 Simulation of electron distribution and stopping power in polyimide film by Casino (a) distribution (b) energy loss.

electrons, hit the sample surface with the energy of 500 keV. The result was shown in Fig. 17. From Fig. 17(a), we can conclude that, due to the high energy, the electrons statistically penetrated the polyimide films, which has the thickness of only 25 μm. However, the penetrating electron could still activate the atoms along its trajectory, as shown in Fig. 17(b), which depicted that, the stopping power in the surface layer is not equal to zero.

Many researchers have devoted to the investigation on high energy electron and proton irradiation on polymer materials. It is summarized that, the injected high energy particles can induced free radicals inside the materials[11-14]. Thus, the un-bonded electron in the free radical is considered to enhance the generation of the secondary electron and photoelectron. Our previous research on the ultraviolet irradiation on total electron emission yield proved to be the same tendency. However, the PEY of electron irradiation polyimide film decreased with the rising of electron irradiation dose, which infers, there exists other degradation effects besides of the generation of free radicals. Finally, the yield variation tendency is the compromise of all the degradation effects. In one word, the further research on the degradation effect is expected by other analysis methods.

The total electron emission yield and photoelectron emission yield of polyimide films degraded by thermal cycles and temperature dependent emission yield are planned to perform in the future investigation.

6. Conclusions

Space environmental aging effect on the total electron emission yield and photoelectron emission yield has been investigated by exposing polyimide film (Kapton 100H) to high energy electron and proton. According to experimental results and analysis, we can summarize three points as below.

(1) The total electron emission yield of polyimide increases with the rising fluence of electron irradiation, while it keeps invariant after the proton exposure.

(2) The photoelectron emission yield of polyimide decreases with the rising fluence of electron irradiation but increases with the rising fluence of proton irradiation.

(3) The penetrated electrons and trapped protons in this research can generate the free radicals, which is considered to affect the electron emission property.

References

1) S. T. Lai: *Fundamentals of Spacecraft Charging: Spacecraft Interactions with Space Plasmas*, Princeton University Press, 2011.
2) D. Hastings et al: *Space Environment Interaction*, Cambridge University Press, 1996.
3) G. F. Dionne: Origin of secondary-electron-emission yield-curve parameters, *J. Appl. Phys.*, vol. 46, no. 8(1975), pp. 3347-3351.
4) Y. Chen et al: Total electron emission yield measurement of insulator by a scanning small detector, *Appl. Phys. Lett.*, vol. 99(2011), p. 152101.
5) J. R. Dennison et al: Evolution of the electron yield curves of insulators as a function of impinging electron fluence and energy, *IEEE Trans. Plasma Sci.*, vol. 34, no. 5(2006), pp. 2204-2218.
6) Y. Chen et al: Photoelectron emission yield measurement of insulator by vacuum ultraviolet light source and several narrow bandwidth filters, presented at 12th Spacecraft Charging Technology Conference, Kitakyushu, Japan, May 13-18, 2012.
7) K. Nomura et al: Measurement system of the development of the photoelectron emission on the spacecraft materials, presented at 12th Spacecraft Charging Technology Conference, Kitakyushu, Japan, May 13-18, 2012.
8) N. Balcon *et al*: Secondary electron emission on space materials: evaluation of the total secondary electron yield from surface potential measurements, *IEEE Trans. Plasma Sci.*, vol. 40, no. 2(2012), pp282-290.
9) M. A. Furman et al: Probabilistic model for the simulation of secondary electron emission, *Phys. Rev. ST Accel. Beams*, 5(2002), p.124404.
10) B. Feuerbacher et al: Experimental investigation of photoemission from satellite surface materials, *J. Appl. Phys.*, vol. 43(1972).
11) C. Y. Sun et al: Investigation on the recombination kinetics of the pyrolytic free-radicals in the irradiated polyimide, *Nuclear Instruments and Methods in Physics Research B*, vol. 271(2012), pp. 61-64.
12) L. Yue et al: Investigation on the radiation induced conductivity of space-applied polyimide under cyclic electron irradiation, *Nuclear Instruments and Methods in Physics Research B*, vol. 291(2012), pp.17-21.
13) R. Artiaga et al: Dynamical mechanical analysis of proton beam irradiated polyimide, *Nuclear Instruments and Methods in Research B*, vol. 236(2005), pp.432-436.
14) Y. Y. Wu et al: A study on the free-radical evolution and its correlation with the optical degradation of 170 keV proton-irradiated polyimide, *Polymer Degradation and Stability*, vol. 95(2010), pp.1219-1225.